Relaxation oscillations and canards of a regulated two-gene model

DE MAESSCHALCK, Peter; Kiss, G & Kovacs, A (2021) Relaxation oscillations and canards of a regulated two-gene model. In: Journal of mathematical analysis and applications (Print), 502 (1) (Art N° 125144).

DOI: 10.1016/j.jmaa.2021.125144
Handle: http://hdl.handle.net/1942/36297

Relaxation oscillations and canards of a regulated two–gene model

P. De Maesschalck G. Kiss A. Kovacs

Abstract

We investigate a two–gene system with an autoregulatory feedback loop using geometric singular perturbation theory. We identify (coexisting) relaxation oscillations, singular Hopf bifurcations, homoclinic loops etc. We also demonstrate a new method to compute the criticality of the singular Hopf bifurcations.

1 Introduction

Gene expression is the vital mechanism to make and maintain living organisms. This paper contributes to the understanding of a mathematical model of gene expression, featuring both stable and bistable scenarios. Understanding such gene expression processes makes the development of novel treatments of various diseases possible, and exposes the way malfunctioning gene expression might lead to tumorigenesis [1]. Bistability in gene expression for instance has been identified as one of the key mechanisms bacteria employ to cope with environmental challenges, such as antibiotic treatment [2, 3]. Hence, a deeper understanding is needed to combat different microbial response mechanisms allowing pathogenic cells to grow slowly at an elevated concentration of antibiotics (antimicrobial resistance) or to switch to an evolutionary developed dormant phenotype (antimicrobial tolerance) [4]. Furthermore, living organisms show cyclic changes in their vital processes timed by their internal circadian clocks. The behaviour of circadian clocks externally affected by cyclic environmental signals, so-called zeitgebers. On the other hand, mutations of genes affecting development and function of circadian clocks could lead to changes in significant features of those oscillations [5]. Therefore, since relation between the internal clocks and zeitgebers impacts drastically human health [6], it is important to understand the nature of oscillations in gene expression. The possibility of influencing circadian period of cyanobacteria is reported in [7].

Gene-regulatory circuits have been used in modelling various aspects of gene expression, see [8, 9] and [10], and the references therein. Our work is motivated by [11] where the singularly perturbed delay differential equation

$$\begin{aligned} \dot{p}(t) &= -k_p p(t) + \frac{k_1}{q(t)+k_2}, \\ \epsilon\dot{q}(t) &= -k_q q(t) + \frac{q^2(t)}{q^2(t)+k_4} p(t-\tau) + k_3 \end{aligned} \tag{1}$$

was proposed as a simplified two-gene model. Here, the parameter $\epsilon > 0$ separates the time scales on which proteins p and q are produced by genes P and Q, respectively. More specifically, in (1) protein p is produced faster than q. Also, $\tau > 0$ is introduced to incorporate the time needed for transcription, translation and translocation processes. Furthermore, positive parameters k_q and k_4, together with the non–negative parameters $k_p,\ k_1,\ k_2,\ k_3$, describe the effects of various aspects of gene expression. In [11], the effect of time delay is investigated on the stability region and the period of the oscillations. Namely, it was shown – mostly numerically – that periodic oscillations can exist for a larger set of parameters when time delays are incorporated compared to the case of the system without delay. Addition of time delay to the models hence makes them much more realistic. It is our ambition to use mathematical tools to give a qualitative description of this time-delayed model, specifically for small delay, but have come to the understanding that in order to do so we will have to rely on specific properties of the non-delayed version. (Even if ultimately one resorts to using numerical methods in the study of the model with delay, one can benefit from an accurate qualitative description of the version with $\tau = 0$.) We will more precisely be interested in the onset of the cycles (Hopf bifurcations), as it will be the starting point to identify parameter regions in the system with delay where cycles are present. In this manuscript, we therefore investigate the non–delayed (1), thereby focusing on using qualitative techniques: the results that we obtain are rigorously proven, with the side-note that for some computations the aid of a computer algebra program was used. Though we are fully aware that the behaviour of the model for $\tau = 0$ has limited use by itself, we will foremost use it as a stepping stone towards the more difficult case $\tau > 0$, relatively small.

Singularly perturbed ordinary differential equations are used in modelling various real world phenomena - biological processes [12], in particular - when system variables are evolving on different time scales. Also, the dynamics of singularly perturbed ordinary differential equations is studied extensively both theoretically, [13, 14], and numerically, [15, 16]. On

the other hand, delay differential equations are also used to formulate descriptive and predictive models of various physical and biological processes when the evolution of a system is significantly affected by its earlier states, [17, 18]. However, although many sophisticated mathematical and computational tools have been developed to study these infinite dimensional dynamical systems, [19, 20], there is no comprehensive geometric theory to study the dynamics of singularly perturbed delay differential equations. Hence, we do not attempt to study (1) here, instead, we set $\tau = 0$. Also, we use the substitution $t = \frac{s}{\epsilon}$, and then denote $\frac{s}{\epsilon}$ by t to get

$$\begin{aligned} \dot{p}(t) &= \epsilon \left(-k_p p(t) + \frac{k_1}{q(t) + k_2} \right), \\ \dot{q}(t) &= -k_q q(t) + \frac{q^2(t)}{q^2(t) + k_4} p(t) + k_3. \end{aligned} \tag{2}$$

The purpose of this paper is to provide as detailed analytically verified description of the dynamics of (2) as possible. This analysis can serve as base in understanding the effects of time delay on the dynamics of (2). The paper is organised as follows. In Section 2, we study the singular limit $\epsilon = 0$ of (2) to derive its bifurcation structure. Also, we obtain results on the number and stability properties of possible equilibria in terms of system parameters. In Section 3, we describe the dynamics of (2) in the (k_1, k_2) parameter space for $\epsilon > 0$ sufficiently small. In Section 4, we study stability properties of periodic orbits, the criticality of the Hopf bifurcation giving birth to those orbits. By computing the stability of the cycles at the bifurcation point and confirming the stability properties of the large relaxation cycles, we can delimit parameter regions for which during the growth of the cycle from bifurcation point to full relaxation cycle there are no changes of stability to be expected (that could lead to saddle-node of limit cycles bifurcations), though at present we have no formal proof of this fact. See the discussion section for futher remarks.

2 Slow-fast analysis - singular bifurcation diagram

We will use geometric singular perturbation theory to study the system. It basically consists of identifying two limiting systems associated to (2): the fast and the slow system. Both give meaningful information at the limit $\epsilon = 0$. Geometric singular perturbation theory (GSPT) combines the information from both limiting systems to provide a qualitative understanding of the dynamics of (2) for nonzero values of $\epsilon > 0$, but keeping ϵ sufficiently

small. We will see below that in one parameter region, the application of GSPT is quite standard, because of the presence of a normally hyperbolically attracting curve; in that case there is a global attractor and there are no periodic movements. In a second parameter region, the dynamics is more interesting as the curve of singular points of the fast subsystem looses normal hyperbolicity at two points. It is the typical framework where one can spot periodic movements of relaxation oscillation type. The geometric analysis is more involved now because a thorough analysis is needed of the points where normal hyperbolicity is lost. In many applications, one typically refers to [21] to identify the nature of the mentioned points; in this paper we present an alternative, more direct way, bypassing the need to put the system in a normal form. It is based on the recent monograph [22].

The analysis below deals with (2), restricted to the first quadrant $p \geq 0$, $q \geq 0$.

Remark 1. *Linear rescalings of (q, p, t, ϵ) preserve the structure of the equations, conditional to an equation to be verified in terms of the scaling factors, and it is easily seen that the value*

$$\kappa = 3\frac{k_3}{k_q}\sqrt{3/k_4} \tag{3}$$

is invariant under such scalings. (The $3\sqrt{3}$ factor will reveal to be convenient later on.) In fact, employing these degrees of freedom, we may assume $k_p = k_q = 1$ and $k_4 = 3$. It means also that we can rewrite k_3 as $\frac{1}{3}k_q\kappa$. In the proof of some properties we will use this simplification, we have preferred to avoid it when presenting results in order to keep the variables and parameters in the presentation as close as possible to their biologically meaningful origin.

2.1 The fast subsystem

The fast subsystem is obtained by putting $\epsilon = 0$ in (2). The singular points of (2), for $\epsilon = 0$, form the so-called critical set $\mathcal{C}_0 = \{(q, p) \in \mathbb{R}^+ \times \mathbb{R}^+ : f(q, p) = 0\}$, with $f(q, p) = -k_q q + \frac{q^2}{q^2+k_4}p + k_3$. In fact, the critical set is a graph, called the critical curve, given by $p = p_1(q)$, where

$$p_1 : \mathbb{R}^+ \to \mathbb{R}, \quad q \mapsto \frac{(k_q q - k_3)(q^2 + k_4)}{q^2}.$$

Note that

(i) $\lim_{q\to\infty} p_1(q) = \infty$;

(ii) $\lim_{q\to 0^+} p_1(q) = -\infty$;

(iii) We will restrict the domain of p_1 to $[q_{min}, \infty[$, in order for the image of p_1 to be inside $\mathbb{R}^+$. We have

$$q_{min} = k_3/k_q.$$

(In view of Remark 1 we may assume $q_{min} = \frac{1}{3}\kappa$.)

The phase plane analysis for (2) in the (q,p)-plane is hence easy for $\epsilon = 0$: the dynamics is in horizontal direction away from or towards the critical set. In fact, it is the sign of the nontrivial eigenvalue

$$D_q f(q_0, p_0), \qquad (q_0, p_0) \in \mathcal{C}_0$$

that distinguishes the attracting behaviour from the repelling behaviour. At points $(q_0, p_0) \in \mathcal{C}_0$ for which this eigenvalue is nonzero, the system is said to be normally hyperbolic. In the other case, eg. the value is zero, the point is called a contact point of the system (because the tangent vector of the critical curve at that point is horizontal and has a first-order contact with the horizontal fibers of the unperturbed dynamics).

Remark 2. *The stability properties of the points on $\mathcal{C}_0$ are related to the sign of*

$$D_q f|_{\mathcal{C}_0} = -\frac{2k_3k_4 - k_4k_q q + k_q q^3}{k_4 q + q^3}, \tag{4}$$

and equivalently to the sign of the numerator of this expression. Fortunately the bifurcation diagram of roots of such a cubic is well-known. Consider a cubic equation

$$x^3 + Bx + C = 0, \tag{5}$$

and let $\Delta = -4B^3 - 27C^2$ be the discriminant of this cubic polynomial. Then $\Delta > 0$ corresponds to the case of three distinct real roots, $\Delta < 0$ to the case of one real root and two distinct complex conjugated roots. When $\Delta = 0$ and $(B, C) \neq (0, 0)$, there are exactly two real roots, one of them with multiplicity 2, when $\Delta = B = C = 0$, there is a single real root with multiplicity 3. A general cubic equation $x^3 + Ax^2 + Bx + C = 0$ can easily be transformed to a similar form with vanishing x^2 coefficient, but in view of the expression for $D_q f$ above, we will not need to do so in this paper and we can directly use the form (5). In the case of positive discriminant, we mention Viètes formula for the roots

$$x = 2\sqrt{\frac{-B}{3}} \cos\left(\frac{1}{3}\arccos\left(\frac{3C}{2B}\sqrt{\frac{-3}{B}}\right) + \frac{2\pi n}{3}\right), \qquad n = -1, 0, 1.$$

The following is a sufficient condition for the existence of a unique, biologically meaningful equilibrium.

Proposition 1. *Let $k_3,\ k_4$ and k_q be given such that*

$$\kappa > 1,$$

where κ is defined in (3). Then, for any given $k_1,\ k_2$ and k_p, $\mathcal{C}_0$ is normally hyperbolic everywhere. That is,

$$D_q f|_{\mathcal{C}_0} \neq 0.$$

Proof. Using (4), we have to find solutions of $k_q q^3 - k_4 k_q q + 2k_3 k_4 = 0$. Clearly, our assumption corresponds to the case $\Delta < 0$ in Remark 2, with $(B, C) = (-k_4, \frac{2k_3 k_4}{k_q})$. From Remark 2 we get that there is a unique real (and simple) solution. Note that the left hand side of the cubic equation changes sign between $q = 0$ and $q = -\infty$, so by the intermediate value theorem the unique solution must be obtained for $q < 0$. □

Proposition 2. *Let $k_3,\ k_4$ and k_q be given such that*

$$0 \leq \kappa < 1. \tag{6}$$

Then there are exactly two points $(q^\ell, p^\ell), (q^r, p^r) \in \mathcal{C}_0$ where normal hyperbolicity is lost. These points are so-called contact points of contact order 2, meaning that

$$D_q f|_{\mathcal{C}_0} = 0, \qquad D^2_{qq} f\big|_{\mathcal{C}_0} \neq 0.$$

at the points. Furthermore, the two points split the critical curve $\mathcal{C}_0$ in three normally hyperbolic parts

$$\begin{aligned}
\mathcal{C}_0^{al} &= \mathcal{C}_0 \cap \left\{(q,p) \in \mathbb{R}^+ \times \mathbb{R} : q_{min} \leq q < q^\ell\right\}, \\
\mathcal{C}_0^{r} &= \mathcal{C}_0 \cap \left\{(q,p) \in \mathbb{R}^+ \times \mathbb{R} : q^\ell < q < q^r\right\}, \\
\mathcal{C}_0^{ar} &= \mathcal{C}_0 \cap \left\{(q,p) \in \mathbb{R}^+ \times \mathbb{R} : q > q^r\right\}.
\end{aligned}$$

Here, $\mathcal{C}_0^{al}$ and $\mathcal{C}_0^{ar}$ are normally hyperbolically attractive, and $\mathcal{C}_0^{ar}$ is normally hyperbolically repelling.

Proof. Similarly to the proof of Proposition 1, we relate the condition in the proposition to $\Delta > 0$ in Remark 2, indicating 3 distinct real solutions of the cubic equation $k_q q^3 - k_4 k_q q + 2k_3 k_4 = 0$. Also similar is the fact that at least one of the three solutions is for $q < 0$. We use the explicit form of

the solutions from Viètes formula (reminding that $(B, C) = (-k_4, \frac{2k_3k_4}{k_q})$): define

$$q = 2\sqrt{\frac{k_4}{3}}\cos\left(\phi + \frac{2\pi n}{3}\right), \qquad n = 0, 1, -1, \qquad \text{with } \phi := \frac{1}{3}\arccos(-\kappa).$$

Notice that our assumption on κ implies that ϕ is a real angle between $\pi/6$ and $\pi/3$. So

$$\phi_0 := \phi \in \left[\tfrac{\pi}{6}, \tfrac{\pi}{3}\right], \quad \phi_1 := \phi + \tfrac{2\pi}{3} \in \left[\tfrac{5\pi}{6}, \pi\right], \quad \phi_{-1} := \phi - \tfrac{2\pi}{3} \in \left[-\tfrac{\pi}{2}, -\tfrac{\pi}{3}\right].$$

The root corresponding to $n = 1$ hence is the one with negative q. Noticing also that $\cos\phi_0 > \cos\phi_{-1}$, we define q^ℓ to be the solution corresponding to $n = -1$ and q^r to be the solution corresponding to $n = 0$; this way $0 < q^\ell < q^r$.

Observe now that it is also possible to solve the equation $D_q f = 0$ w.r.t. k_4. We then find $k_4 = \frac{k_q q^3}{k_q q - 2k_3}$. When $q \le q_{min} = k_3/k_q$, the expression for k_4 becomes negative. This easy computation actually shows that under the condition of this proposition, we necessarily have $q^\ell > q_{min}$.

To exclude the possibility of flex points on the critical curve, we will prove that the presence of a solution of the system $\{f = D_q f = D^2_{qq} f = 0\}$ implies that $\kappa = 1$. We have

$$D_q f = -k_q + \frac{2k_4 pq}{(q^2 + k_4)^2}, \qquad D^2_{qq} f = \frac{2k_4 p(k_4 - 3q^2)}{(q^2 + k_4)^3}.$$

It is a bit cumbersome to solve this set of 3 equations; as a guideline to the reader, we mention that it is best to consider $\{D_q f = D^2_{qq} f = 0\}$ as a system of equations in $\{q, k_4\}$, solve it by hand and substitute the solution in $f = 0$. Solving this third equation and substituting it back in the expression for k_4 leads to concluding that $\kappa = 1$. As a consequence, under the condition $\kappa < 1$, at all contact points that were found above, the second order derivative is nonzero. Since $D^2_{qq} f \to -\infty$ as $q \to \infty$, the branch $\mathcal{C}_0^{ar}$ is attracting. It implies the stability properties along the other branches, keeping in mind that q^ℓ and q^r are contact points of contact order 2. □

Remark 3. *Following Remark 1, we have*

$$k_3 = \frac{\kappa k_q}{3}, \qquad \kappa = -\cos(3\phi), \qquad q^\ell = 2\cos(\phi - 2\pi/3), \qquad q^r = 2\cos\phi$$

so we might as well use (k_1, k_2, ϕ) as bifurcation parameters instead of the parameters (k_1, k_2, k_3) (remember that we have $k_p = k_q = 1$ and $k_4 = 3$).

Reducing the fast system

In the language of vector fields, we have

$$X = \left(-k_q q + \frac{pq^2}{q^2+k_4} + k_3\right)\frac{\partial}{\partial q} + \epsilon\left(-k_p p + \frac{k_1}{q+k_2}\right)\frac{\partial}{\partial p}.$$

Following [22] we write $X = F.Z + \epsilon Q$ with

$$F = k_q q^3 - (k_3+p)q^2 + k_4 k_q q - k_3 k_4, \qquad Z = \frac{-1}{q^2+k_4}\frac{\partial}{\partial q},$$

and

$$Q = \left(-k_p p + \frac{k_1}{q+k_2}\right)\frac{\partial}{\partial p}.$$

Remark 4. *Clearly there are multiple ways to decompose X into $FZ + \epsilon Q$: a factor can be multiplied to F provided one divides Q with the same factor. This will not cause any difficulties.*

In the next section, we will use this decomposition to further analyse the slow-fast system.

2.2 The slow subsystem

Traditionally, the slow subsystem is derived in the following way. One first rescales time in (2) to find

$$p'(s) = \left(-k_p p(s) + \frac{k_1}{q(s)+k_2}\right),$$
$$\epsilon q'(s) = -k_q q(s) + \frac{q^2(s)}{q^2(s)+k_4}p(s) + k_3,$$

and then considers the unperturbed system by setting $\epsilon = 0$ to get

$$0 = -k_q q(s) + \frac{q^2(s)}{q^2(s)+k_4}p(s) + k_3,$$
$$p'(s) = -k_p p(s) + \frac{k_1}{q(s)+k_2}.$$

This dynamical system is only defined along the normally hyperbolic parts of the critical curve $p = p_1(q)$. Given the fact that the curve is a parameterized curve by the parameter q, it is better to write it as

$$p = p_1(q(s)),$$
$$p_1'(q(s))q'(s) = -k_p p(s) + \frac{k_1}{q(s)+k_2}.$$

Proposition 3. *The slow flow, which is restricted to* $\mathcal{C}_0 \setminus \{(q^\ell, p^\ell), (q^r, p^r)\}$, *is*

$$q' = \frac{-k_p(k_q q - k_3)(q^2 + k_4)(q + k_2) + k_1 q^2}{q^2(q + k_2)} \times \frac{q^3}{k_q q^3 - k_4 k_q q + 2k_3 k_4}. \quad (7)$$

Proof. Straightforward computations. □

The rest of the subsection is concerned with the study of singular points in the slow dynamics, under the condition $\kappa < 1$. The quartic equation for the singularities

$$-k_p(k_q q - k_3)(q^2 + k_4)(q + k_2) + k_1 q^2$$

has at least one root on $]-\infty, q_{min}[$ and at least one root on $]q_{min}, \infty[$, as can be learned from the intermediate value theorem. So the number of roots on $q > q_{min}$ lies between 1 and 3.

Lemma 1. *Given* $q_2 \in]q_\ell, q_r[$, *there is a double singularity of the slow dynamics at* $q = q_2$ *along the parameter values*

$$(k_1, k_2) = \left(\tfrac{k_p}{q_2} \tfrac{(q_2^2+k_4)^2(k_3-k_q q_2)^2}{k_4 k_q q_2 - k_q q_2^3 - 2k_3 k_4},\ q_2 \tfrac{k_3 k_4 - k_3 q_2^2 + 2k_q q_2^3}{k_4 k_q q_2 - k_q q_2^3 - 2k_3 k_4} \right). \quad (8)$$

For other values of q_2 *or away from that parameter locus, singularities of the slow dynamics are simple. Both* k_1 *and* k_2 *tend to* $+\infty$ *as* q_2 *approaches* q_ℓ *or* q_r. *The double singularity is actually a triple singularity at some* $q = q_3(k_3)$. *Fixing all parameters but* k_1 *and* k_2, *the locus in the* (k_1, k_2)*-plane of double singularities of the slow dynamics is a union of two graphs of* k_1 *(with positive slope), on* $[k_1^3, \infty[$, *and both graphs meet at the point where the triple singularity is located.*

Proof. It is a tedious exercise to find the double roots of the slow dynamics in (7), leading to (8). Since the sign of k_1 is the same as the sign of $k_4 k_q q_2 - k_q q_2^3 - 2k_3 k_4$, the latter expression should be positive, which corresponds to the denominator in the expression for k_2. So also the numerator in the expression for k_2 should be positive, and this is only true along the middle (repelling) branch.

A computation shows the presence of a triple root at $q = q_3$ for any choice of $q_3 \in]q_{min}, \sqrt{k_4/3}[$ at the parameter values

$$(k_1, k_2, k_3) = \left(\tfrac{k_p k_q}{k_4} \tfrac{(q_3^2+k_4)^3}{k_4 - 3q_3^2},\ \sqrt{\tfrac{3}{k_4}} \tfrac{q_3^2(q_3+\sqrt{3k_4})}{\sqrt{3k_4}-3q_3},\ k_q \sqrt{\tfrac{3}{k_4}} \tfrac{q_3^2(\sqrt{3k_4}-q_3)}{\sqrt{3k_4}+3q_3} \right).$$

One can verify that

$$\frac{\partial k_3}{\partial q_3} = \frac{6\sqrt{3}k_q}{\sqrt{k_4}} q_3 \frac{k_4 - q_3^2}{(\sqrt{3k_4} + 3q)^2} > 0.$$

So we can invert $k_3 = k_3(q_3)$ and write it as $q_3 = q_3(k_3)$. Denote by k_1^3 the k_1-value at that specific point. Let us now turn our attention again towards the double singularities. Notice that in the expression (8), we have

$$\frac{\partial k_1}{\partial q_2} = -2k_p k_q \frac{(q_2^2+k_4)(q_2-q_{min})}{q_2^2(k_4 k_q q_2 - k_q q_2^3 - 2k_3 k_4)^2} \times \\ (k_q q_2^3 + \sqrt{3k_4} k_q q_2^2 - \sqrt{3k_4} k_3 q_2 + k_3 k_4)(k_q q_2^3 - \sqrt{3k_4} k_q q_2^2 + \sqrt{3k_4} k_3 q_2 + k_3 k_4).$$

All factors except for the last two are clearly nonzero. The second to last is also nonzero: to see this one Taylor expands the expression about $q = q_{min}$:

$$k_q q_2^3 + \sqrt{3k_4} k_q q_2^2 - \sqrt{3k_4} k_3 q_2 + k_3 k_4 = k_q (q_2 - q_{min})^3 + (\sqrt{3k_4} k_q + 3k_3)(q_2 - q_{min})^2 \\ + \frac{k_3(\sqrt{3k_4} k_q + 3k_3)}{k_q}(q_2 - q_{min}) + k_3 \frac{k_4 k_q^2 + k_3^2}{k_q^2}.$$

The last factor in $\frac{\partial k_3}{\partial q_3}$ does have a zero, precisely at $q_2 = q_3(k_3)$, which can be checked by plugging the expression for the triple point into the expression of $\frac{\partial k_3}{\partial q_3}$. It is a simple zero and the only one: the derivative w.r.t. q_2 of this last factor has a Taylor expansion about $q = q_{min}$ with all strictly positive coefficients (we need to use $\kappa \leq 1$ here).

This analysis shows that the double-singularity curve, parameterized by q_2, can be split in two components: one for $q_\ell < q_2 < q_3(k_3)$ and one for $q_3(k_3) < q_2 < q_r$. Both components can be expressed as a graph $k_2 = k_2(k_1)$ (and $q_2 = q_2(k_1)$, with $k_1 \geq k_1^3$. Finally, a lengthy computation shows that

$$\frac{\partial k_2}{\partial k_1} = \frac{\left.\frac{\partial k_2}{\partial q_2}\right|_{q_2 = q_2(k_1)}}{\left.\frac{\partial k_1}{\partial q_2}\right|_{q_2 = q_2(k_1)}} = k_p \frac{q_2^2 + k_4}{q_2^2}(q_2 - q_{min})\Big|_{q_2 = q_2(k_1)} > 0.$$

It shows that the slope of both curves is strictly positive. By checking (with some computations) that the derivative w.r.t. q_2 of the right-hand side of this expression is negative, we conclude that the graph that corresponds to $q_\ell < q_2 < q_3(k_3)$ lies above the graph that corresponds to $q_3(k_3) < q_2 < q_r$. □

2.3 Analysis of the contact points

The dynamics near contact points depends on the nature of the contact point. We distinguish jump points, slow-fast Hopf points (or turning point), slow-fast Bogdanov-Takens points, ... The classification of contact points is based on the so-called contact order (order of contact between the fast fibers and the critical curve) and singularity order (order of zero of the slow dynamics). These notions can be observed after putting the system in normal form, but we present here ready-to-use formulas that do not require the system to be put in normal form and that can be used directly to distinguish a jump point from a slow-fast Hopf point. We make use of the language of vector fields as before and write $X = FZ + \epsilon Q$.

Proposition 4 ([22])**.** *For a contact point of contact order 2, the expression $Q(F)$ (eg. applying the vector field Q as a Lie derivative of the function F) is nonzero if and only if the contact point is a jump point. In the other case, the expression $[Z, Q](F)$ (eg. applying the Lie Bracket of Z and Q to the function F) is strictly negative if and only if the contact point is a slow-fast Hopf point.*

Remark 5. *(1) A similar coordinate-free criterion for slow-fast Hopf points can be found in [23]. (2) The formula can be explained as follows: near a contact point, the expressions F and $Z(F)$ form a regular coordinate system, F corresponding to the fast variable and $Z(F)$ to the slow variable. The vector field Q can be seen as the slow vector field, and in that sense it is natural to expect that $Q(F)$ can be used to characterize the singularity at the fold. Similarly $Q(Z(F))$ can be seen as the "slow derivative" of the slow variable $Z(F)$. In most expressions $Z(Q(F)) = 0$, so $Q(Z(F)) = [Z, Q](F)$.*

So let us compute $Q(F)$, $Z(F)$ and $[Z, Q](F)$:

$$\begin{aligned} Q(F) &= \left(-k_p p + \frac{k_1}{q + k_2}\right) \frac{\partial}{\partial p} \left(k_q q^3 - (k_3 + p)q^2 + k_4 k_q q - k_3 k_4\right) \\ &= \left(k_p p - \frac{k_1}{q + k_2}\right) q^2, \\ Z(F) &= \frac{-3k_q q^2 + 2k_3 q - k_4 k_q + 2pq}{q^2 + k_4}, \end{aligned}$$

and

$$\begin{aligned} [Z, Q](F) &= Z(Q(F)) - Q(Z(F)) \\ &= -\frac{k_1 q^2}{(q^2 + k_4)(q + k_2)^2} < 0. \end{aligned}$$

We conclude that the contact points are either jump points (eg. when $Q(F) \neq 0$) or slow-fast Hopf points (when $Q(F) = 0$). Using the expression for $Q(F)$ above and writing $p = p_1(q)$ in it we find

Proposition 5. *Let (q^*, p^*) be a contact point, i.e. $* \in \{\ell, r\}$. Then the contact point is a jump point whenever*

$$k_1 \neq k_1^* := k_p \frac{((q^*)^2 + k_4)(q^* + k_2)(k_q q^* - k_3)}{(q^*)^2}.$$

(Recall that the expression of q^* does not depend on k_1.) The locus $k_1 = k_1^\ell$ will be denoted by SH_ℓ; the locus $k_1 = k_1^r$ will be denoted by SH_r. (The acronym stands for singular Hopf; at this point we have only established the presence of singular contact points, see the next section for details.)

The slow-fast Hopf parameter curves SH_ℓ and SH_r are given by $k_1 = k_1^\ell$ (with $q = q^\ell$) and $k_1 = k_1^r$ (with $q = q^r$). Note that q^ℓ and q^r do not depend on k_1 or k_2. Notice also that

$$\frac{\partial k_1^*}{\partial k_2} = k_p k_q \frac{(q^*)^2 + k_4}{(q^*)^2}(q^* - q_{min}) > 0$$

so both curves are also curves $k_2 = k_2^*(k_1)$ with positive slope. By checking the derivative w.r.t. q^* of this expression it can be seen that the slope of the SH_ℓ curve is smaller than the slow of the SH_r curve.

Following Remark 2 and choosing $k_4 = 3$ and $k_p = k_q = 1$, we find

$$k_1^r = \tfrac{1}{12} \tfrac{(\cos(3\phi)+6\cos\phi)(4\cos^2\phi+3)(2\cos\phi+k_2)}{\cos^2\phi}$$

at $q = q^r$ and

$$k_1^\ell = \tfrac{1}{12} \tfrac{(\cos(3\phi)+6\cos(\phi-2\pi/3))(4\cos^2(\phi-2\pi/3)+3)(2\cos(\phi-2\pi/3)+k_2)}{\cos^2(\phi-2\pi/3)}$$

at $q = q^\ell$.

Proposition 6. *There is a locus $\mathrm{SH}_{\ell r}$*

$$k_2 = k_2^*(k_3) = 2\frac{k_q q^\ell q^r (q^\ell + q^r) + k_3(k_4 - q^\ell q^r)}{k_q (q^r - q^\ell)^2}.$$

When $k_2 = k_2^*$, the values k_1^ℓ and k_1^r coincide. For $k_2 < k_2^*$ we have $k_1^\ell < k_1^r$ and vice-versa for $k_2 > k_2^*$. Along $k_2 = k_2^*$ we have $k_1^\ell = k_1^r$. Alternatively, the $\mathrm{SH}_{\ell r}$ curve can be parameterized by ϕ.

Note: it is not so hard to show that $q^\ell q^r < k_4$, implying that $k_2^* > 0$.

Proposition 7. *The* $\mathrm{SH}_{\ell r}$ *point lies inside the* SN*-wedge. The upper* SN *branch intersects* SH_ℓ *exactly once at a point* SN_ℓ *(and it does not intersect* SH_r*). The lower* SN *branch intersects* SH_r *exactly once at a point* SN_r *(and it does not intersect* SH_r*).*

Proof. Outside the SN wedge there is only one singular point, so definitely $\mathrm{SH}_{\ell r}$ lies inside. Since we know the slope of both Hopf curves is different, the union of their graphs is a topological cross, and the triple point T lies in the quadrant to the left of the crossing, between the two curves. Since to the left of T, the parameters are outside the wedge, it implies that both Hopf curves must intersect the SN curve at least once to the left of the crossing of the Hopf curves. Let us now compute the slope of the parametric SN-curve. The slope is given by

$$\frac{\partial k_2}{\partial q} \Big/ \frac{\partial k_1}{\partial q} = \frac{q^2}{k_p(q - q_{min})(q^2 + k_4)}.$$

We can learn two things from this expression: (1) when evaluated at $q = q_*$, with $* \in \{\ell, r\}$, it coincides with the slope of the curve $k_1 = k_1^*$ (or more precisely, this curve written as a graph expressing k_2 in terms of k_1). Also as q goes from q_ℓ to q_r, this slope changes monotonically. Recall also that q_ℓ and q_r are independent of k_1 and k_2. So it means that the SN curve is nowhere parallel to the Hopf curves. Rolle's theorem excludes multiple intersections in that case. The fact that the upper branch of SN does not intersect the SH_r curve originates from the same reasoning: the upper branch has a slope that is always higher than that of the SH_r curve. The argument is similar for the non-intersection of the lower branch of SN with SH_ℓ. □

2.4 Singular bifurcation diagram

With the information from the previous sections we can explain the bifurcation diagram in Fig. 1 to a large extent. Under the assumption $\kappa < 1$, the critical curve has two extremes, a left one and a right one, so in this regime the shape of the critical curve does not bifurcate. However, the intersections of the critical curve with the isocline $\dot{p} = 0$, which determine the singular points of the slow vector field, does behave differently upon varying parameters.

First we distinguish two parameter curves $k_1 = k_1^\ell$ and $k_1 = k_1^r$, along which respectively the left and the right contact point is singular. We denote

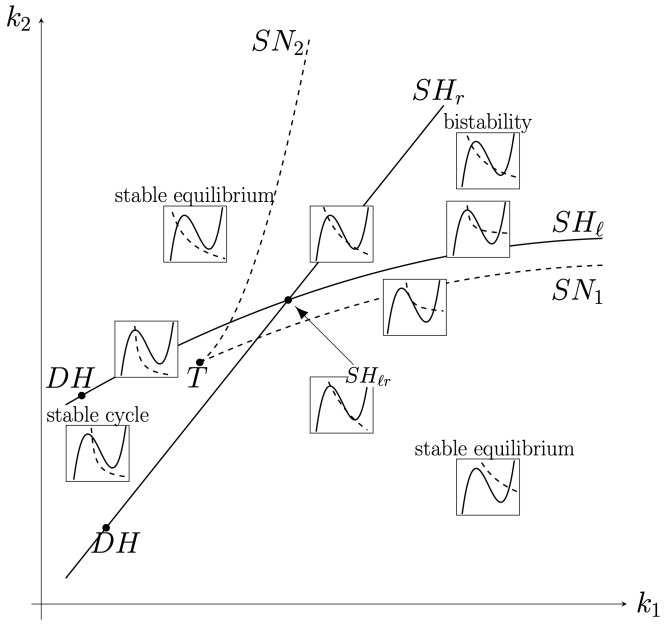

Figure 1: Singular bifurcations in parameter space (k_1, k_2), keeping κ (or equivalently k_3) fixed.

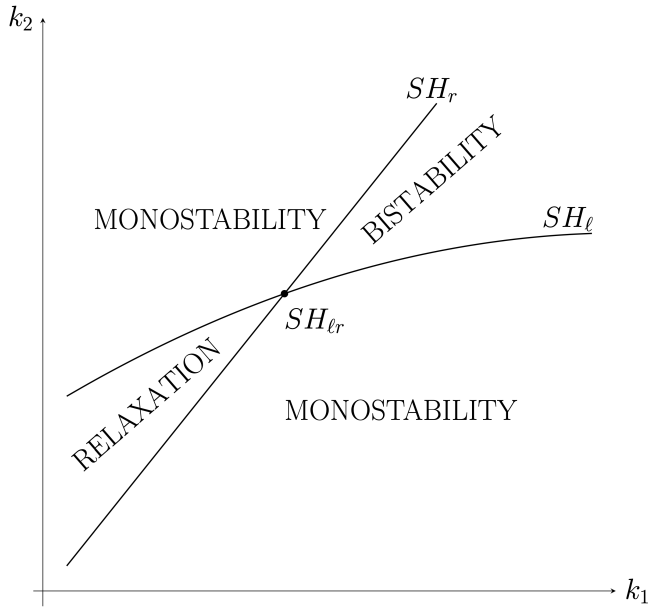

Figure 2: Singular Hopf curves separate 4 regions with distinguished behaviour

these loci by SH_ℓ and SH_r. (The acronym stands for singular Hopf; at this point we have only established the presence of singular contact points, see the next section for details.) Their intersection is denoted as $\mathrm{SH}_{\ell r}$ in Figure 1; it is a point.

3 Behaviour away from SH_ℓ and SH_r

In the (k_1, k_2)-plane, and for fixed other parameter values, the singular Hopf curves SH_ℓ and SH_r form a cross and define 4 regions, see Fig. 2

(R1) Relaxation oscillation region: below SH_ℓ and above SH_r.

(R2) Bistability region: below SH_r and above SH_ℓ.

(R3) 2 Monostability regions: either above both or below both curves.

Proposition 8. *Given parameters (k_1, k_2) in the relaxation oscillation region (R1). Then for $\epsilon > 0$ sufficiently small there is one limit cycle which is*

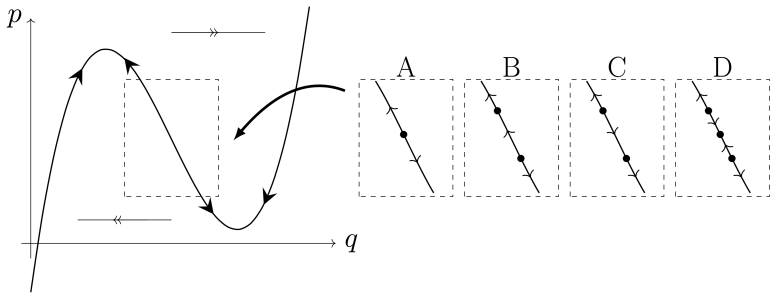

Figure 3: Behaviour in the relaxation-oscillation region, for sufficiently small $\epsilon > 0$. The behaviour near the unstable branch of the critical curve depends on whether (k_1, k_2) lies in or out the SN-wedge, but it is of little importance for the global dynamics

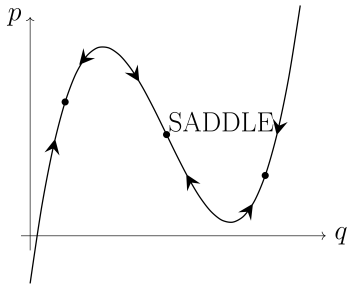

Figure 4: Behaviour in the bistability region, for sufficiently small $\epsilon > 0$.

stable and which surrounds 1–3 singularities counted with multiplicity. (See Figure 3.)

Proof. This is a classic application of a result in singular perturbations. In this parameter region, the slow flow only has singular points on the middle branch, and the two contact points are jump points. It is a hyperbolically attracting slow-fast cycle, called a "*common*" cycle in [24]. Of course, earlier works dealt with these kind of oscillations as well, see [25] or [26] for example. □

Proposition 9. *Given parameters (k_1, k_2) in the bistability region (R2). Then for $\epsilon > 0$ sufficiently small there are no limit cycles and there are 3 singularities. Two are stable nodes and one is of saddle type. (See Figure 4.)*

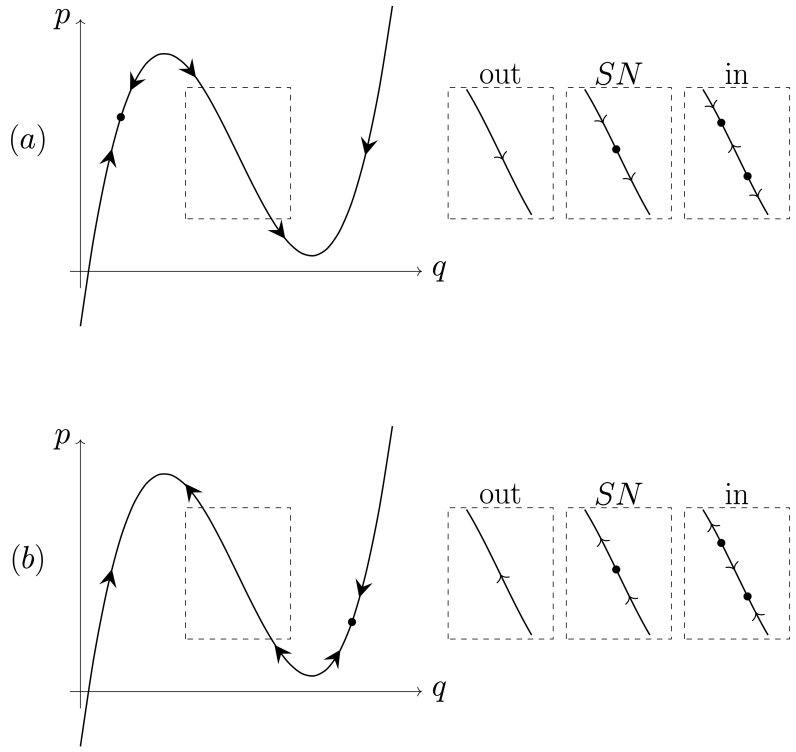

Figure 5: Behaviour in the monostability regions, for sufficiently small $\epsilon > 0$.

Proof. It is elementary to construct an ϵ-family of trapping regions surrounding the three singular points, in a way that the dynamics in the (q, p)-plane is globally attracted towards the inside of this region. Inside the region it is elementary to conclude the results. □

Proposition 10. *Given parameters (k_1, k_2) in a monostability region (R3). Then for $\epsilon > 0$ sufficiently small there are no limit cycles and there is a stable singularity. At most two other singularities are present, of saddle type or unstable node type.(See Figure 5.)*

Proof. Similar to the reasoning in the proof of Proposition 9. □

3.1 Slow-fast Hopf bifurcations

Proposition 11 ([22])**.** *Let $X_\lambda = F_\lambda X_\lambda + \epsilon Q_\lambda$ have a contact point of contact order 2, for all λ close to some λ_0. If the contact point is a slow-fast*

Hopf point for $\lambda = \lambda_0$ (see Proposition 4 for a criterion), and if furthermore

$$\frac{\partial}{\partial \lambda} Q_\lambda(F_\lambda)\Big|_{\lambda=\lambda_0} \neq 0$$

then a slow-fast Hopf bifurcation takes place w.r.t. λ at λ_0.

It is clear that both k_1 and k_2 can play the role of such a bifurcation parameter λ along the bifurcation curves SH_ℓ and SH_r. Moreover, although this is not explicitly proved in [22], the fact that

$$\begin{vmatrix} \frac{\partial}{\partial k_1} Q(F)|_{q=q^\ell} & \frac{\partial}{\partial k_2} Q(F)|_{q=q^\ell} \\ \frac{\partial}{\partial k_1} Q(F)|_{q=q^r} & \frac{\partial}{\partial k_2} Q(F)|_{q=q^r} \end{vmatrix} \neq 0$$

allows to prove the simultaneity of both bifurcations along $\mathrm{SH}_{\ell r}$.

3.1.1 Slow-fast Hopf bifurcations outside the wedge formed by SN

Outside the wedge formed by SN, there is only one singular point, which is the slow-fast Hopf point. What we then observe, say on a point of SH_ℓ, is a classical so-called canard explosion: a rapid increase of amplitude of the limit cycle, accompanied by a quick change in the shape: from canard without head to canard with head, much like in the classical Van der Pol case, see Fig. 6.

Unlike in the Van der Pol case, the limit cycle here may not be unique, and need not necessarily be stable. The stability at the onset of the bifurcation will be studied in Section 4, and it will become clear from that analysis that bifurcations in the criticality are present. To control the stability and possible unicity of limit cycles further on during the canard explosion, i.e. when the limit cycle approaches a canard cycle of certain height, one needs to compute a so-called slow divergence integral. It is beyond the scope of what we wanted to do in this paper.

3.1.2 Slow-fast Hopf bifurcations inside the wedge formed by SN

Inside the wedge, and along SH_ℓ or SH_r, there is at least one singular point on the middle branch of the critical curve. What we then observe, say on a point of SH_ℓ, is a so-called truncated canard explosion. The stability at the onset of the canard explosion is again studied in Section 4, where we will see that the bifurcation is always subcritical, meaning an unstable cycle is

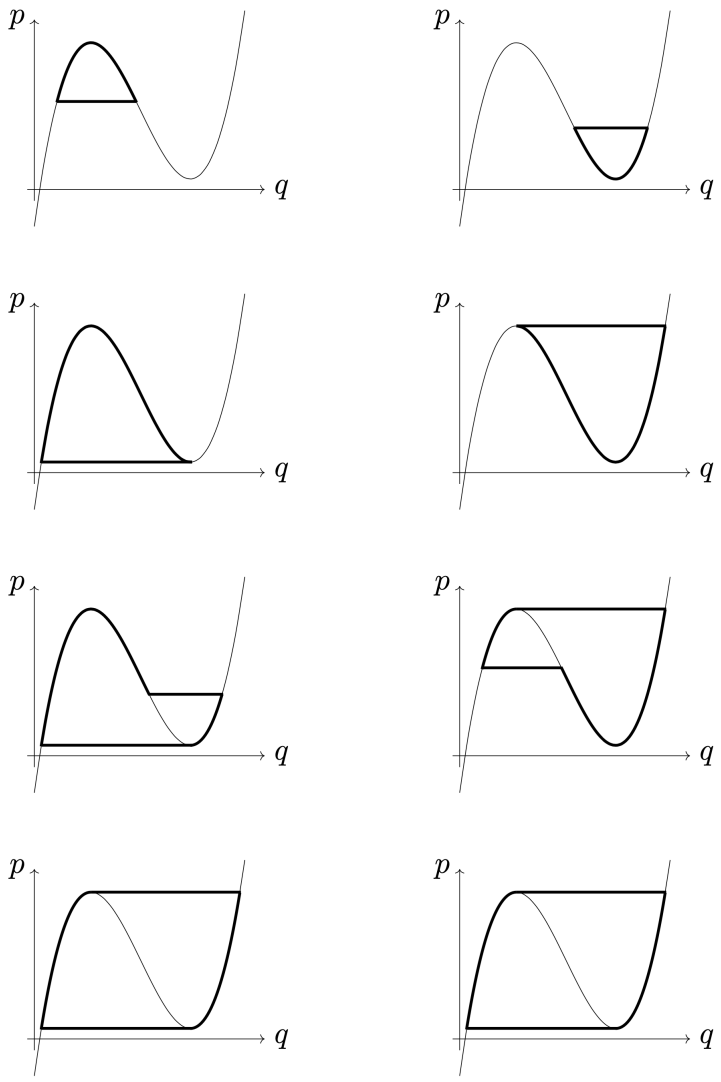

Figure 6: Canard explosion: quick change from small cycle to big cycle, with intermediate shape changes from headless canard to canard with head. (a) canard explosion along SH_ℓ, (b) canard explosion along SH_r.

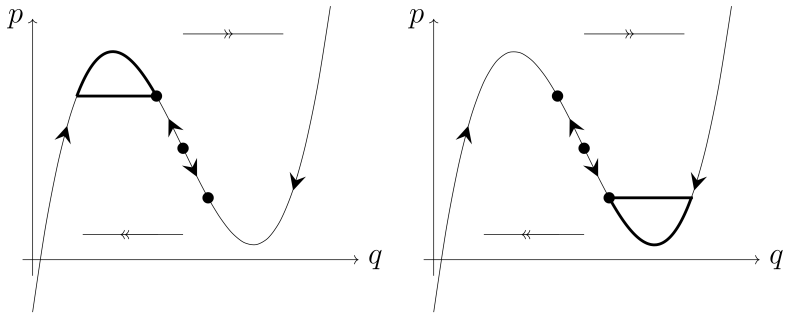

Figure 7: Truncated canard explosion: quick change from small cycle to big cycle, ending at a canard-type homoclinic orbit. (a) homoclinic near SH_ℓ, (b) homoclinic near SH_r.

born. We claim — without proof — that the unstable behaviour of the cycle is maintained along the canard explosion up until the end point. The end of the truncated canard explosion is where the unstable cycle grows into a saddle homoclinic, the saddle being the singularity near the middle branch of the critical curve. See Figure 7.

The proof of existence of canard-type homoclinics can for example be found in [27]. Note that because the saddle singularity is on the unstable branch, this causes the nearby periodic orbits of canard type to be hyperbolically unstable, this can be deduced from the results in [27].

3.1.3 Slow-fast Hopf bifurcations on $\mathrm{SN} \cap (\mathrm{SH}_\ell \cup \mathrm{SH}_r)$

On the SN-locus, a saddle-node type singularity is found in the slow dynamics. Just like in the previous case, a homoclinic canard-type orbit is found; we again refer to [27] for details on a method of proof.

4 Criticality of the singular Hopf bifurcations

In case of a slow-fast Hopf point, it still has to be determined which criticality the Hopf bifurcation has (sub-critical versus super-critical, or degenerate Hopf). The relaxation parameter regime in Fig. 2 is delimited by two singular Hopf curves. Of course it is important to realize that the figure is made for $\epsilon = 0$. If one were to picture the full diagram with a vertical ϵ axis on top of the picture, a singular Hopf curve would be the vertex of an exponentially small wedge inside which canard cycles are observed. These

cycles are not necessarily stable. In fact the stability of small such cycles is governed by the criticality of the Hopf bifurcation. In most occasions in this model the criticality will point out that the canard cycles are unstable from the onset. In that case, one automatically finds saddle-node of limit cycles as one approaches the boundary of the exponentially small wedge. Dynamically it means that inside the relaxation-type cycle there is a region delimited by an unstable canard-type cycle. The canard cycle separates the basin of attraction of the relaxation cycle from the basin of attraction of the singular (focus) point. It may be relevant in applications to point out that in these models the relaxation cycle is not a global attractor in all cases, but that in some spurious "canard" cases, part of the phase space will not be attracted to the cycle.

One method to compute the criticality is to bring the system in normal form and compute the first Lyapunov coefficient using [21], but it reveals that the normal form computation is not so easy. We have opted to use the intrinsic formula for the Lyapunov coefficient found in [28]. Of course, computations are unavoidable also in this case, but they are manageable. Let us describe the result of [28] using the decomposition $X = FZ + \epsilon Q$. To that end, a first ingredient is the scalar

$$\mathcal{A} = \frac{Z^3(F)}{Z^2(F)^2}.$$

Here, $Z^2(F)$ and $Z^3(F)$ are iterated evaluations of the Lie derivative of F w.r.t. the vector field Z; the additional superscript 2 in the denominator is just a square. Second ingredient is

$$\mathcal{G} = \Omega(Q, Z).\Omega(\nabla F, \nabla(ZF)).$$

Here, ∇ is the gradient of a function, in our case $\nabla F = (\frac{\partial F}{\partial q}, \frac{\partial F}{\partial p})$, because we chose to work in the (q, p)-plane. It is shown in [28] that it does not matter in which coordinates the gradient is being computed. Ω is an area form in general, but in our case it is just the determinant of a matrix where the two vectors are written as columns. (Should one want to compute the gradient in different coordinates, then the area form needs to be adapted accordingly.) Third ingredient is the unique vector field V that satisfies

$$V(F) = 0, \qquad V(Z(F)) = 1.$$

Theorem 1. *[28] If at a slow-fast Hopf point at which a slow-fast Hopf bifurcation takes place, the value of*

$$\sigma := \frac{1}{2}V^2(\mathcal{G}) - V(\mathcal{G})\mathcal{A}$$

is strictly positive, then the Hopf bifurcation is subcritical, when it is negative, the bifurcation is supercritical. When $\sigma = 0$, a degenerate slow-fast Hopf bifurcation takes place of at least degeneracy order two.

Computing $\mathcal{A}$

We have

$$\begin{aligned} Z(F) &= \frac{-3k_q q^2 + 2k_3 q - k_4 k_q + 2pq}{q^2 + k_4}, \\ Z^2(F) &= 2\frac{k_3 q^2 + 2k_4 k_q q + pq^2 - k_3 k_4 - k_4 p}{(q^2 + k_4)^3}, \\ Z^3(F) &= 4\frac{2k_3 q^3 + 5k_4 k_q q^2 + 2pq^3 - 4k_3 k_4 q - k_4^2 k_q - 4k_4 pq}{(q^2 + k_4)^5}. \end{aligned}$$

At a singular contact point 3 conditions are satisfied:

$$F = 0, \qquad Z(F) = 0, \qquad Q(F) = 0.$$

Instead of solving the equations w.r.t. the phase variables it reveals convenient to solve the system w.r.t. (p, k_1, k_3):

$$p = \frac{k_q(q^2 + k_4)^2}{2k_4 q}, \quad k_1 = \frac{k_p k_q (q + k_2)(q^2 + k_4)^2}{2k_4 q}, \quad k_3 = \frac{k_q q(k_4 - q^2)}{2k_4}. \tag{9}$$

Evaluating the expressions at a singular contact point simplifies them:

$$Z(F) = 0, \quad Z^2(F) = -k_q \frac{k_4 - 3q^2}{q(q^2 + k_4)^2} \quad Z^3(F) = -12k_q \frac{k_4 - q^2}{(q^2 + k_4)^4}.$$

This leads to the following expression for $\mathcal{A}$:

$$\mathcal{A} = -12q^2 \frac{k_4 - q^2}{k_q(k_4 - 3q^2)^2}.$$

Computing $\mathcal{G}$

Next, we compute $\mathcal{G}$. Using $\nabla = (\frac{\partial}{\partial q}, \frac{\partial}{\partial p})$, we first calculate

$$\begin{aligned} \Omega(\nabla F, \nabla ZF) &= \begin{vmatrix} 3k_q q^2 - 2k_3 q + k_4 k_q - 2pq & 2\frac{-k_3 q^2 - 2k_4 k_q q - pq^2 + k_3 k_4 + k_4 p}{(q^2 + k_4)^2} \\ -q^2 & \frac{2q}{q^2 + k_4} \end{vmatrix} \\ &= -2q\frac{-3k_q q^4 + 3k_3 q^3 - 2k_4 k_q q^2 + 3pq^3 + k_3 k_4 q - k_4^2 k_q + k_4 pq}{(q^2 + k_4)^2} \\ &= 2k_4 \frac{-2k_q q^3 + 3k_3 q^2 + k_3 k_4}{(q^2 + k_4)^2}, \end{aligned}$$

where we have replaced p in the last expression by the value for p that solves $F = 0$. We may do so since $\mathcal{G}$ is defined up to $O(F)$. We also need

$$\begin{aligned}\Omega(Q,Z) &= \begin{vmatrix} 0 & -\frac{1}{q^2+k_4} \\ -k_p p + \frac{k_1}{q+k_2} & 0 \end{vmatrix} \\ &= \frac{-k_2 k_p p - k_p p q + k_1}{(q+k_2)(q^2+k_4)}.\end{aligned}$$

We have not substituted p here because it actually makes the formula more complicated. So from the above considerations we find

$$\begin{aligned}\mathcal{G} &= \Omega(\nabla F, \nabla ZF)\Omega(Q,Z) \\ &= 2k_4 \frac{-2k_q q^3 + 3k_3 q^2 + k_3 k_4}{(q^2+k_4)^2} . \frac{-k_2 k_p p - k_p p q + k_1}{(q+k_2)(q^2+k_4)}.\end{aligned}$$

Computing the vector field / differential operator V

It is elementary to check that

$$V := \tfrac{(q^2+k_4)^2}{2k_4(-2k_q q^3+3k_3 q^2+k_3 k_4)} \left(q^2 \tfrac{\partial}{\partial q} + (3k_q q^2 - 2k_3 q + k_4 k_q - 2pq) \tfrac{\partial}{\partial p} \right)$$

is the unique vector field for which $V(F) = 0$ and $V(Z(F)) = 1$. Note that V, evaluated at a contact point, eg. using (9), simplifies to

$$V = \frac{q(q^2+k_4)}{k_q(k_4-3q^2)} \frac{\partial}{\partial q}.$$

Similarly,

$$V^2 = V \circ V = \tfrac{2q(q^2+k_4)(k_4^2+3k_4 q^2-6q^4)}{k_q^2(k_4-3q^2)^3} \tfrac{\partial}{\partial q} - \tfrac{(q^2+k_4)^2}{k_q q(k_4-3q^2)} \tfrac{\partial}{\partial p} + \tfrac{q^2(q^2+k_4)^2}{k_q^2(k_4-3q^2)^2} \tfrac{\partial^2}{\partial q^2}.$$

Computing the first Lyapunov constant σ

Using the expression for V at a contact point, we easily find

$$V(\mathcal{G}) = -k_p k_q \frac{q(q^2+k_4)}{2k_4(q+k_2)}.$$

And a bit more involved computation (preferably aided by some computer algebra program) leads to

$$\begin{aligned}V^2(\mathcal{G}) = k_p \tfrac{k_2^2 k_4^3 + k_2 k_4^3 q + k_4^2(k_4-6k_2^2)q^2 - 4k_2 k_4^2 q^3 + k_4(9k_2^2+k_4)q^4}{k_4(k_4-3q^2)^2(q+k_2)^2} \\ + k_p \tfrac{21k_2 k_4 q^5 + 7k_4 q^6 - 6k_2 q^7 - 9q^8}{k_4(k_4-3q^2)^2(q+k_2)^2}.\end{aligned}$$

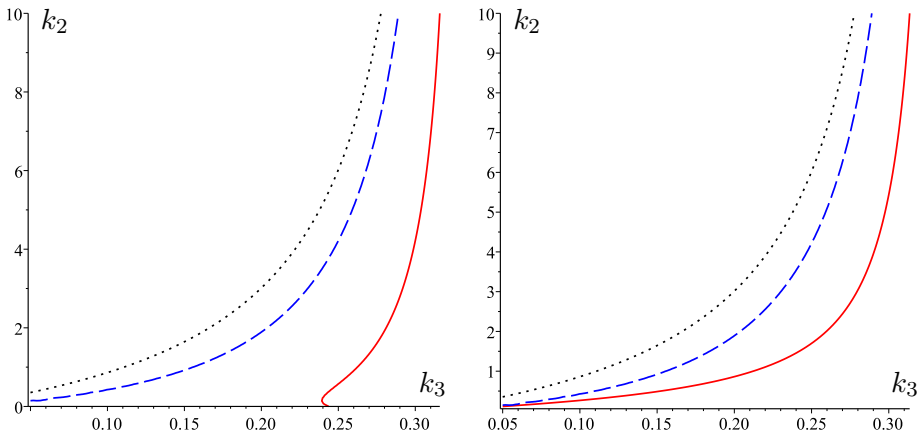

Figure 8: (k_3-families of) special points on SH_ℓ (left) and SH_r (right). The dotted line is $\mathrm{SH}_{\ell r}$. The dashed curve is SN (the inside of the wedge is to the left of it). The solid line is the zero set of σ, i.e. the degenerate Hopf point. Below of the solid line, the Hopf bifurcations are supercritical, elsewhere the Hopf bifurcations are subcritical.

Putting all things together we find

$$\sigma = k_p \frac{\bar{\sigma}(k_2, k_4, q)}{2(q+k_2)^2(k_4 - 3q^2)^2}$$

where

$$\bar{\sigma}(k_2, k_4, q) := k_4(k_4 - 3q^2)^2 k_2^2 + q(6q^6 + 21k_4q^4 - 16k_4^2q^2 + k_4^3)k_2 + (3q^8 + 7k_4q^6 - 11k_4^2q^4 + k_4^3q^2).$$

In Figure 8, we show the zero set of σ. From the picture it can be seen that any degenerate Hopf point lies outside the SN wedge. For all values of k_3 there is a change in criticality along the SH_r branch, also for sufficiently large values of k_3 this happens on the SH_ℓ branch.

Remark 6. *On the majority of the* SH_ℓ *and* SH_r *branches, the Hopf bifurcations render unstable cycles. It means that for the relaxation cycle in the nearby relaxation-oscillation region will collapse together with the rapidly growing canard cycle in a saddle-node of limit cycles (SNLC) bifurcation. As one moves along* SH_ℓ *or* SH_r *in increasing* k_2 *direction, starting from the double Hopf point, the amplitude of the SNLC will grow up to the* SN *locus. The detailed study of the SNLC bifurcation involves computing slow divergence integrals and go beyond the scope of this paper.*

5 Discussion

In this paper, using geometric singular perturbation theory, we described the dynamics of (2) in the (k_1, k_2) parameter space. In particular, we identified a region where the model possesses co-existing stable equilibria. Also, we established the existence of relaxation oscillations, stable limit cycles surrounding singularities. Last but not least, we gave a detailed description of the transition process starting with small periodic orbits and resulting in relaxation oscillations. It is important to remark that although this transition is developing in a very narrow range of the bifurcation parameter, it may have long lasting effects. For instance, if dynamics affecting parameters are changing slowly, for instance as a result of prolonged ageing processes, the system can spend a considerable amount of time in the canard explosion regime. Therefore, it is crucial to understand the dynamical properties of these small oscillations. When determining stability properties of canard solutions, to avoid the challenging and lengthy computations of normal form reduction, we used a novel method presented in [28].

The stability of relaxation cycles, if present, are clear from the analysis: they are always (strongly) stable. It is much less clear for the canard cycles. This paper shows the extent to which one can compute the stability of such cycles analytically in a realistic manner: we have obtained a formula in closed form expressing the stability of the Hopf bifurcation, but it reveals not possible without reverting to numerics to track the saddle-node of canard limit cycles further away from the Hopf point. To do so one would have to compute the so-called slow-divergence integrals, but computations were found to be too cumbersome. From the criticality computations we are nevertheless able to infer that in the canard region the relaxation cycle is not globally stable as the interior of the coexisting unstable canard cycle is attracted to the singular point instead.

References

[1] Joan Massagué. TGFβ in cancer. *Cell*, 134(2):215 – 230, 2008.

[2] David Dubnau and Richard Losick. Bistability in bacteria. *Molecular microbiology*, 61(3):564–572, 2006.

[3] Markus Arnoldini, Ima Avalos Vizcarra, Rafael Peña-Miller, Nicolas Stocker, Médéric Diard, Viola Vogel, Robert E. Beardmore, Wolf-Dietrich Hardt, and Martin Ackermann. Bistable expression of viru-

lence genes in salmonella leads to the formation of an antibiotic-tolerant subpopulation. *PLOS Biology*, 12(8):1–8, 08 2014.

[4] Kim Lewis. Persister cells, dormancy and infectious disease. *Nature Reviews Microbiology*, 5(1):48, 2007.

[5] Ronald J Konopka and Seymour Benzer. Clock mutants of drosophila melanogaster. *Proceedings of the National Academy of Sciences*, 68(9):2112–2116, 1971.

[6] Till Roenneberg and Martha Merrow. The circadian clock and human health. *Current biology*, 26(10):R432–R443, 2016.

[7] Kumiko Ito-Miwa, Yoshihiko Furuike, Shuji Akiyama, and Takao Kondo. Tuning the circadian period of cyanobacteria up to 6.6 days by the single amino acid substitutions in kaic. *Proceedings of the National Academy of Sciences*, 117(34):20926–20931, 2020.

[8] Timothy S. Gardner, Charles R. Cantor, and James J. Collins. Construction of a genetic toggle switch in escherichia coli. *Nature*, 403:339 EP –, 01 2000.

[9] Uri Alon. *An introduction to systems biology: design principles of biological circuits*. Chapman and Hall/CRC, 2006.

[10] Luonan Chen, Ruiqi Wang, Chunguang Li, and Kazuyuki Aihara. *Modeling biomolecular networks in cells: structures and dynamics*. Springer Science & Business Media, 2010.

[11] Luonan Chen and Kazuyuki Aihara. A model of periodic oscillation for genetic regulatory systems. *IEEE Transactions on Circuits and Systems I: Fundamental Theory and Applications*, 49(10):1429–1436, 2002.

[12] Geertje Hek. Geometric singular perturbation theory in biological practice. *Journal of Mathematical Biology*, 60(3):347–386, Mar 2010.

[13] Christian Kuehn. *Multiple time scale dynamics*, volume 191. Springer, 2015.

[14] Christopher K. R. T. Jones. Geometric singular perturbation theory. In *Dynamical systems (Montecatini Terme, 1994)*, volume 1609 of *Lecture Notes in Math.*, pages 44–118. Springer, Berlin, 1995.

[15] Mathieu Desroches, John Guckenheimer, Bernd Krauskopf, Christian Kuehn, Hinke M Osinga, and Martin Wechselberger. Mixed-mode oscillations with multiple time scales. *Siam Review*, 54(2):211–288, 2012.

[16] Peter De Maesschalck and Mathieu Desroches. Numerical continuation techniques for planar slow-fast systems. *SIAM Journal on Applied Dynamical Systems*, 12(3):1159–1180, 2013.

[17] Thomas Erneux. *Applied delay differential equations*, volume 3. Springer Science & Business Media, 2009.

[18] Hal L Smith. *An introduction to delay differential equations with applications to the life sciences*, volume 57. Springer New York, 2011.

[19] Ovide Arino, Moulay Lhassan Hbid, and E Ait Dads. *Delay Differential Equations and Applications: Proceedings of the NATO Advanced Study Institute held in Marrakech, Morocco, 9-21 September 2002*, volume 205. Springer Science & Business Media, 2007.

[20] Jack K Hale and Sjoerd M Verduyn Lunel. *Introduction to functional differential equations*, volume 99. Springer Science & Business Media, 2013.

[21] M. Krupa and P. Szmolyan. Relaxation oscillation and canard explosion. *J. Differential Equations*, 174(2):312–368, 2001.

[22] Peter De Maesschalck, Freddy Dumortier, and Robert Roussarie. *Canard cycles from birth to transition*. submitted, 2020.

[23] Martin Wechselberger. *Geometric Singular Perturbation Theory Beyond the Standard Form*. Springer, 2020.

[24] P. De Maesschalck, F. Dumortier, and R. Roussarie. Cyclicity of common slow-fast cycles. *Indag. Math. (N.S.)*, 22(3-4):165–206, 2011.

[25] E. F. Mishchenko, Yu. S. Kolesov, A. Yu. Kolesov, and N. Kh. Rozov. *Asymptotic methods in singularly perturbed systems*. Monographs in Contemporary Mathematics. Consultants Bureau, New York, 1994. Translated from the Russian by Irene Aleksanova.

[26] A. N. Tihonov. Systems of differential equations containing small parameters in the derivatives. *Mat. Sbornik N. S.*, 31(73):575–586, 1952.

[27] P. De Maesschalck and F. Dumortier. Canard cycles in the presence of slow dynamics with singularities. *Proc. Roy. Soc. Edinburgh Sect. A*, 138(2):265–299, 2008.

[28] Peter De Maesschalck, Thai Son Doan, and Jeroen Wynen. Intrinsic determination of the criticality of a slow-fast Hopf bifurcation. *arXiv e-prints*, page arXiv:2005.10742, May 2020.